Video Article

Contrast Enhanced Ultrasound Imaging for Assessment of Spinal Cord Blood Flow in Experimental Spinal Cord Injury

Arnaud Dubory[1,2], Elisabeth Laemmel[1], Anna Badner[3], Jacques Duranteau[1,4], Eric Vicaut[1], Charles Court[2], Marc Soubeyrand[1,2]

[1]Laboratoire d'étude de la microcirculation, Faculté de Médecine Paris Diderot Paris VII, U942

[2]Department of orthopaedic surgery, Bicetre Universitary Hospital, Public Assistance of Paris Hospital

[3]Institute of Medical Science, Faculty of Medicine, University of Toronto

[4]Department of Intensive care and Anesthesiology, Bicetre Universitary Hospital, Public Assistance of Paris Hospital

Correspondence to: Marc Soubeyrand at soubeyrand.marc@gmail.com

URL: http://www.jove.com/video/52536
DOI: doi:10.3791/52536

Keywords: Medicine, Issue 99, Spinal cord blood flow, ischemia, spinal cord injury, contrast enhanced ultrasound, rat, contrast agent, Sonovue

Date Published: 5/7/2015

Citation: Dubory, A., Laemmel, E., Badner, A., Duranteau, J., Vicaut, E., Court, C., Soubeyrand, M. Contrast Enhanced Ultrasound Imaging for Assessment of Spinal Cord Blood Flow in Experimental Spinal Cord Injury. *J. Vis. Exp.* (99), e52536, doi:10.3791/52536 (2015).

Abstract

Reduced spinal cord blood flow (SCBF) (*i.e.,* ischemia) plays a key role in traumatic spinal cord injury (SCI) pathophysiology and is accordingly an important target for neuroprotective therapies. Although several techniques have been described to assess SCBF, they all have significant limitations. To overcome the latter, we propose the use of real-time contrast enhanced ultrasound imaging (CEU). Here we describe the application of this technique in a rat contusion model of SCI. A jugular catheter is first implanted for the repeated injection of contrast agent, a sodium chloride solution of sulphur hexafluoride encapsulated microbubbles. The spine is then stabilized with a custom-made 3D-frame and the spinal cord dura mater is exposed by a laminectomy at ThIX-ThXII. The ultrasound probe is then positioned at the posterior aspect of the dura mater (coated with ultrasound gel). To assess baseline SCBF, a single intravenous injection (400 µl) of contrast agent is applied to record its passage through the intact spinal cord microvasculature. A weight-drop device is subsequently used to generate a reproducible experimental contusion model of SCI. Contrast agent is re-injected 15 min following the injury to assess post-SCI SCBF changes. CEU allows for real time and *in-vivo* assessment of SCBF changes following SCI. In the uninjured animal, ultrasound imaging showed uneven blood flow along the intact spinal cord. Furthermore, 15 min post-SCI, there was critical ischemia at the level of the epicenter while SCBF remained preserved in the more remote intact areas. In the regions adjacent to the epicenter (both rostral and caudal), SCBF was significantly reduced. This corresponds to the previously described “ischemic penumbra zone”. This tool is of major interest for assessing the effects of therapies aimed at limiting ischemia and the resulting tissue necrosis subsequent to SCI.

Video Link

The video component of this article can be found at http://www.jove.com/video/52536/

Introduction

Traumatic spinal cord injury (SCI) is a devastating condition leading to significant impairment in motor, sensory and autonomous functions. To date, no therapy has demonstrated its efficiency in patients. For such reason, it is important to identify new techniques that will improve the assessment of potential treatments and can further elucidate injury pathiophysiology[1].

SCI is divided into two sequential phases, referred to as primary and secondary injuries. The primary injury corresponds to the initial mechanical insult. Whereas the secondary injury groups a cascade of various biological events (such as inflammation, oxidative stress and hypoxia) that further contribute to the progressive expansion of the initial lesion, tissue damage and therefore neurological deficit[2,3].

At the acute phase of SCI, neuroprotective therapies are aimed at reducing the secondary injury pathology and should accordingly improve neurological outcomes. Among the many secondary injury events, ischemia plays a crucial role [4,5]. At the level of the SCI epicenter, the damaged parenchymal microvessels impede effective spinal cord blood flow (SCBF). Moreover, SCBF is also significantly reduced in the region surrounding the injury epicenter, an area specifically known as the “ischemic penumbra zone”. If SCBF cannot be quickly restored within these regions, ischemia can lead to supplementary parenchymal necrosis and further nervous tissue damage. As even the slightest tissue preservation can have substantial effects of function, it is of major interest to develop drugs and therapies that can reduce ischemia post-SCI. To highlight this phenomenon, previous work has shown that preservation of only 10% of myelinated axons was enough to permit walking in cats post-SCI [6].

Although several techniques have been described to assess SCBF, they all have significant limitations. For example, the use of radioactive microspheres[7,8] and C14-iodopyrine autoradiography[9] requires subsequent animal sacrifice and cannot be repeated at later time-points. The hydrogen clearance technique[10] depends on the insertion of intraspinal electrodes, which may further damage the spinal cord. While laser Doppler imaging, photoplethysmography[14,15] and *in-vivo* light microscopy[16] have a very limited depth/area of measurement[11-13].

Our team has previously shown that contrast enhanced ultrasound (CEU) imaging can be used to assess real time and *in-vivo* the SCBF changes in the rat spinal cord parenchyma[17]. It is important to note that a similar technique was applied by Huang *et al.* in a porcine model of SCI[18]. CEU applies a specific mode of ultrasound imaging which allows to associate grayscale morphological images (obtained by the conventional B-mode) with spatial distribution of blood flow [19]. The SCBF imaging and quantification relies on intravascular injection of echo-contrast agents. The contrast agent is made up of sulphur hexafluoride microbubbles (mean diameter of about 2.5 µm and 90% having a diameter less than 6 µm) stabilized by phospholipids. The microbubbles reflect the ultrasound beam emitted by the probe thus enhancing blood echogenicity and increasing contrast of the tissues according to their blood flow. It is therefore possible to assess the blood flow in a given region of interest according to the intensity of the reflected signal. The microbubbles are also safe and they have been clinically applied in humans. The sulphur hexafluoride is quickly cleared (mean terminal half-life is 12 min) and more than 80% of the administered sulphur hexafluoride is recovered in exhaled air within 2 min after injection. This protocol provides a simple way to use CEU imaging to assess SCBF changes in rat.

Protocol

NOTE: The methods described in this manuscript were approved by the bioethics committee of the Lariboisière School of Medicine, Paris, France (CEEALV/2011–08-01).

1. Instrument Preparation

1. Prepare and clean the following instruments for catheter insertion: micro-forceps, micro-scissors, micro-vascular clamp, large scissors, surgical thread (Black braided silk 4-0) and a 14 G catheter. Heparinize the catheter with a heparin solution (5,000 U/ml).
2. Prepare and clean the following instruments for the laminectomy: large scissors, scalpel and a bone cutter. Perform laminectomy with a custom-made bone cutter designed to reduce the risk of harming the spinal cord during the laminectomy (**Figure 1**).
3. Set-up the 3D-frame used for positioning and stabilization of the animal. The custom-made frame is built with the elements of an External Fixator Hoffman 3 in association with forceps, which have been curved in order to fit the lumbar spine of the animal.
4. Prepare the weight-drop device (impactor) used for spinal cord biomechanical injury.
   NOTE: The custom-made impaction device was designed with a 3D software and printed in 3D.
5. Turn on the ultrasound machine.
6. Prepare the kit for reconstitution of the contrast agent.
   NOTE: The kit includes 1 vial containing 25 mg of lyophilised powder, 1 pre-filled syringe containing 5 ml sodium chloride and one mini-spike transfer system (**Figure 2**). The steps for reconstitution of the contrast agent are detailed below (in section 5).

2. Jugular Vein Catheterization (Figure 3)

1. *Anesthetize* the animal with 4% isoflurane. Place the animal in supine position. Confirm proper anesthetization by ensuring that the animal is unresponsive when the paws are pinched with a forceps. Apply vet ointment on eyes to prevent dryness while under anesthesia.
2. Shave the neck and clean the skin. Make an incision on the midline of the neck. Retract the sternocleidomastoidian muscle in order to find the internal jugular vein. Tighten a ligature at the rostral part of the vein.
3. Apply a microvascular clamp on the vein, 1 cm below the ligature. Pass another thread around the vein, just below the clamp with the knot ready to be tighten when the clamp is released.
4. Open the wall of vein (venotomy) between the clamp and the rostral ligature. Introduce a 14 G catheter in the lumen of the vein and push it toward the heart.
5. When it comes up against the clamp, release the latter and push the catheter further. Secure the catheter in the vein, by firmly tightening the knot on the vein with the catheter inside.
6. Assess patency of the catheter by withdrawing a small amount of venous blood in the catheter and subsequently then flushing it with heparinized saline. This prevents obstruction of the catheter by a potential blood clot.
7. Connect flexible tubing to the catheter for further injection of contrast agent (microbubbles). Keep it closed (sealed) until ready for use.

3. Accessing the Spine, Laminectomy and Rat Positioning (in the 3D-frame)

1. Place the animal in a flat prone horizontal position. Shave and clean the back (thoracic region) of the animal.
2. Identify the last rib (the XIIIth in the rat) by palpation (**Figure 4**). This allows one to estimate the location of the XIIIth thoracic vertebra (ThXIII).
3. Make a 4 cm skin incision on the midline, centered on ThXIII. Open the skin incision as well as the underlying bursa. Observe the aponeurosis of back muscles as well as the tips of the vertebral spine processes.
4. Carefully localize the spine process of ThXIII by palpating the XIIIth ribs.
   NOTE: The XIIIth rib is connected to ThXIII and therefore represents an easy to locate anatomic landmark for the identification of ThXIII. This step enables the localization of the ThXII to ThIX spinous process as well as L1 and L2 (first and second lumbar vertebras).
5. Cut the muscular aponeurosis and detach the muscles on either side to expose the spinous processes, the laminas and the facet joints from ThIX to L2. Expose the lateral aspects of L1 and L2 by detaching muscles from the transverse processes.
6. Hook the animal's incisor teeth on the 3D-frame to secure the position (**Figure 5**). Clamp the L1 and L2 vertebras with the modified forceps. Connect the modified forceps to the 3D-frame in order to stabilize the animal.
7. Gently pull caudally the forceps holding the lumbar spine in order to tighten the whole spine and to elevate the thorax from the bench.
   NOTE: With the described arrangement the animal should be able to breath. Furthermore, despite respiratory movements of the rib cage, the spine and the spinal cord should also remain immobile.
8. Remove the spinous processess from ThIX to ThXII. Gently insert the inferior blade of the bone cutter beneath the left lamina of ThXII and then close the bone cutter in order to cut the lamina (**Figure 6**).

9. Repeat the same manoeuvre for the right lamina and successively remove the posterior arch. Repeat the previous steps for the vertebras ThXI to ThIX in order to achieve a four-level laminectomy. Remove both facet joints for each vertebra.
   NOTE: Throughout the procedure, clean the operative field from local bleeding. For that, use cotton swabs and irrigation with tepid saline. Hemostasis systematically occurs within minutes.

4. CEU Probe Positioning

1. Cover the dura mater with ultrasound gel. This allows effective transmission of the ultrasound waves between the probe and the spinal cord (**Figure 7**).
2. Stabilize the ultrasound probe with a clamp that can be subsequently connected to the 3D-frame by a jointed arm. Manually position the probe. Ensure that the probe is oriented to obtain an oblique longitudinal sagittal slice. In a correct position, the spinal cord is strictly horizontal on the image and the central canal of the spinal cord is visible along the full segment of the spinal cord.
   NOTE: Positioning should be guided by the real-time B-mode image displayed on the screen of the ultrasound machine. The focal distance of the ultrasound probe should be aligned with the central canal of the spinal cord. At this time, the posterior aspect of the spinal cord is accessible which will ultimately allow for positioning of the impactor.
3. When optimal, lock the jointed arm to stabilize the position.

5. Preparation of Contrast Agent - Microbubble Reconstitution

1. Using the contents of a commercial reconstitution kit and connect the plunger rod by fastening it tightly into the syringe (clockwise). Open the transfer system blister and remove the syringe tip cap. Open the transfer system cap and connect the syringe to the transfer system (fasten tightly).
2. Remove the protective disk from the vial. Slide the vial into the transparent sleeve of the
3. transfer system and press firmly to lock the vial in place.
4. Empty the contents of the syringe into the vial by pushing on the plunger rod. Shake vigorously for 20 sec to mix all the contents in the vial to obtain a white milky homogeneous liquid.
5. Invert the system and carefully withdraw the contrast agent into the syringe. Unscrew the syringe from the transfer system. After reconstitution (as directed), 1 ml of the resulting dispersion contains 8 µl sulphur hexafluoride in the microbubbles. Draw the suspension of microbubbles into a 100 ml syringe. Insert the 100 ml syringe into the electric pump. Close the lid.
6. Start constant agitation of the reconstituted microbubbles. Obtained constant agitation by slow rotation of the syringe, which maintains the microbubble suspension. Connect the pump to the jugular catheter through the flexible tubing. Set the ultrasound machine to “Harmonic Mode”.
   NOTE: The latter corresponds to the mode in which the microbubbles can be specifically detected and visualized. This mode has a low mechanical index, which doesn’t destroy the microbubbles as opposed to the B-mode.
7. Purge the catheter by infusing a first dose (400 µl) of contrast agent. During this first infusion, check that the microbubbles do appear on the ultrasound screen. This confirms that the whole circuit (from the syringe to the rat’s bloodstream) is intact and open.
8. Set the ultrasound machine to “B-mode” to visualize the spinal cord parenchyma and the destruction of the few microbubbles remaining in the bloodstream. The high frequency of the “B-Mode” transmits high energy to the microbubbles, which enables them to breakdown.
9. Let the animal lay still for approximately 30 min. This period allows for the stabilization of the haemodynamic parameters.

6. Assessment of SCBF in the Intact Spinal Cord

1. Set the ultrasound machine to the “Harmonic Mode”. Start simultaneously (1) infusion of contrast agent (400 µl) and (2) the chronometer.
   NOTE: During the infusion, the concentration of microbubbles in the bloodstream should increase, enabling the contrast imagining of the spinal cord (**Figure 8**). Since the microbubbles are quickly destroyed, the blood concentration of microbubbles starts decreasing once the injection is completed which generates a progressive decrease in contrast visualization of the spinal cord.
2. After 1 min, select (press) the “Clip Store” button on the ultrasound machine. This will enable one to save 1 min of raw ultrasound data and the imaging video recording (that was previously displayed on the ultrasound screen).
3. Set the ultrasound machine to “B-Mode”. This will eliminate the remaining microbubbles.

7. Experimental SCI

1. Using the micromanipulator connected to the 3D-frame, position the weight-drop impaction device so that the tip of the impactor comes in contact with the dura mater (on the spinal cord midline), at the junction between ThX and ThXI (**Figure 9**).
   NOTE: This level should correspond to the middle of the segment of spinal cord observed with the ultrasound device. The striker and the body of the impactor are 8 mm in diameter. The tip of the impactor, which will generate the injury, is 3 mm in diameter.
2. Place the striker of the impaction device at a 10 cm-high position. Induce the experimental SCI by releasing the striker of the impaction device. The striker falls and releases the impactor, injuring the spinal cord. The custom made impaction delivers an impact equivalent to a 10 g weight dropped from a height of 10 cm.

8. Assessment of SCBF 5 min Post-SCI

1. Repeat the steps described in section 6 (Assessment of SCBF). The microbubbles will be unable to pass through the damaged microvasculature and the injury epicenter will remain dark (**Figure 10**).

9. Animal Sacrifice

1. Euthanize the animal with intra-peritoneal lethal injection of pentobarbital (100 mg).

10. Quantification of SCBF by Offline Analysis

1. Start the Ultra-Extend Software used for quantification (on ultrasound machine). Select "*file*" and then select previously saved raw data and open the associated files. Activate the "*quantification mode*" by pressing (selecting) the "*Chi Q*" button. Select "*Set ROI*" (button) and choose the circular shape.
2. Select "*Draw ROI*" (button) and draw seven adjacent circular regions of interest (ROI) on the spinal cord (**Figure 11**). Open the menu "*Fitting*" and choose the function "*Curve value*". Observe the software displaying several curves, each corresponding to the changes of microbubbles concentration inside a ROI.
   NOTE: Each curve has a "perfusion-deperfusion" profile. The first phase of the curve is flat and corresponds to the period before the arrival of microbubbles. In the second phase, the concentration of microbubbles quickly increases as a result of the infusion. In the third phase, which begins when the infusion is complete, the concentration of microbubbles progressively decreases as they disintegratse in the bloodstream.
3. Place the first vertical line at the beginning of the second phase of the curve and select "*SET*". This informs the software where to begin analysis.
4. Place the second vertical line at the end of the recording and once again select "*SET*". This informs the software where to stop analysis.
5. Look at the "*Cv*" menu and record the "*AUC*" value, which corresponds to the "*Area Under the Curve*" analyzed. This value is proportional to the SCBF inside the corresponding ROI.

Representative Results

With the protocol described above, it is possible to map the SCBF along a longitudinal spinal cord sagittal segment.

In the intact spinal cord, there appears to be SCBF irregularities within the parenchyma (**Figure 12**). This can be explained by the variable distribution of radiculo-medullary arteries (RMA) from one animal to another. RMA refers to segmental arteries that reach the anterior spinal artery (ASA) and therefore provide blood supply to the spinal cord parenchyma. In contrast, the radicular arteries correspond to segmental arteries, which do not reach the ASA and therefore do not provide spinal cord blood supply. Therefore, in spinal cord segments where the RMA anastomoses with the ASA, there is more blood flow (as shown in our results).

After SCI, real-time CEU imaging shows a deficiency in circulation at the injury epicenter. The epicenter remains dark (no contrast agent signal), as there is no active blood flow. More detailed analysis of the blood flow using several ROIs shows three unique blood flow territories. First, at the level of the epicenter, the blood flow is the lowest with a mean decrease of about -90%. Second, in the territories adjacent to the epicenter (both rostral and caudal), SCBF was also significantly decreased (ranging from -50% to -80%). Third, in the most remote areas corresponding to intact tissue, SCBF is preserved. The second region corresponds to the "ischemic penumbra zone", which should be the target of potential neuroprotective therapies. Being able to readily visualize and quantify SCBF changes post-SCI is useful for assessing the efficiency of therapies aimed at reducing tissue ischemia, and therefore highlights the importance of this technique (**Figure 13**).

Figure 1. The custom-made bone cutter for laminectomies. The thin blade is designed to slide beneath the lamina. Please click here to view a larger version of this figure.

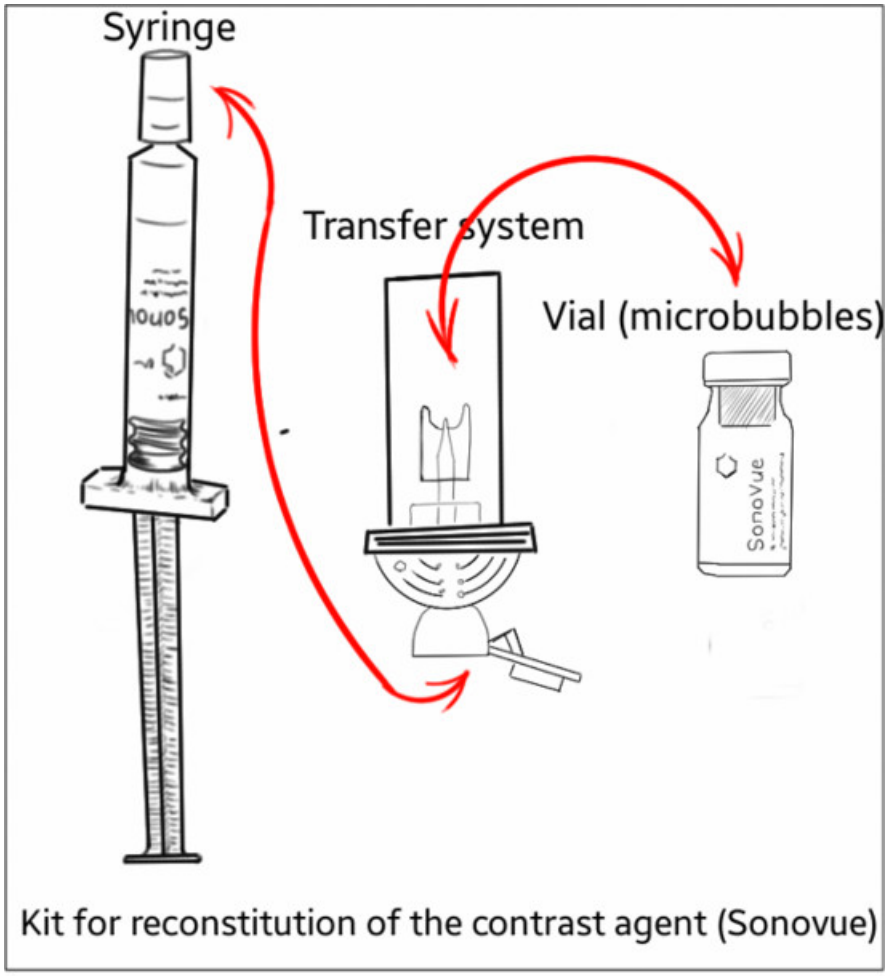

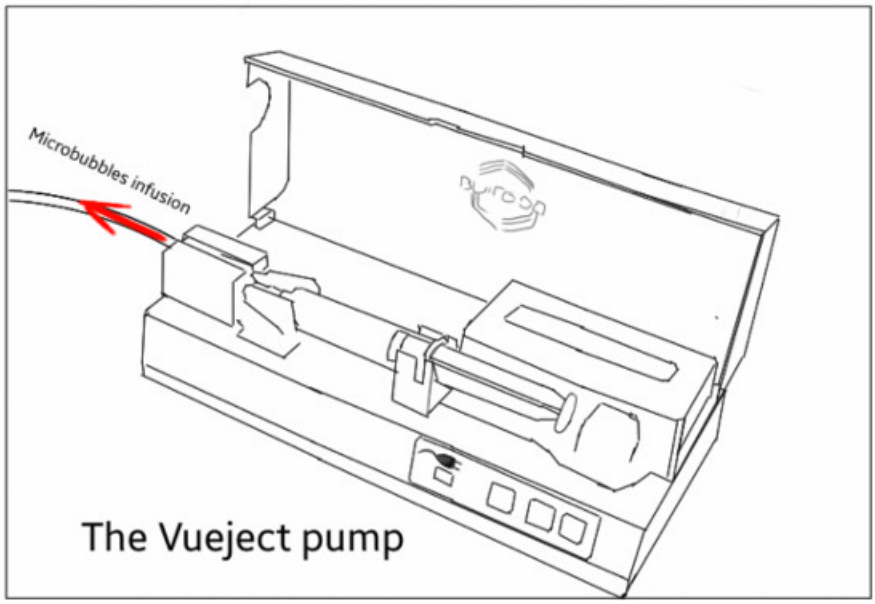

Figure 2. Schematic representation of the kit for microbubbles reconstitution and the Vueject° pump used for microbubbles infusion. The transfer system allows for the delivery of microbubbles and saline between the vial and the syringe. Please click here to view a larger version of this figure.

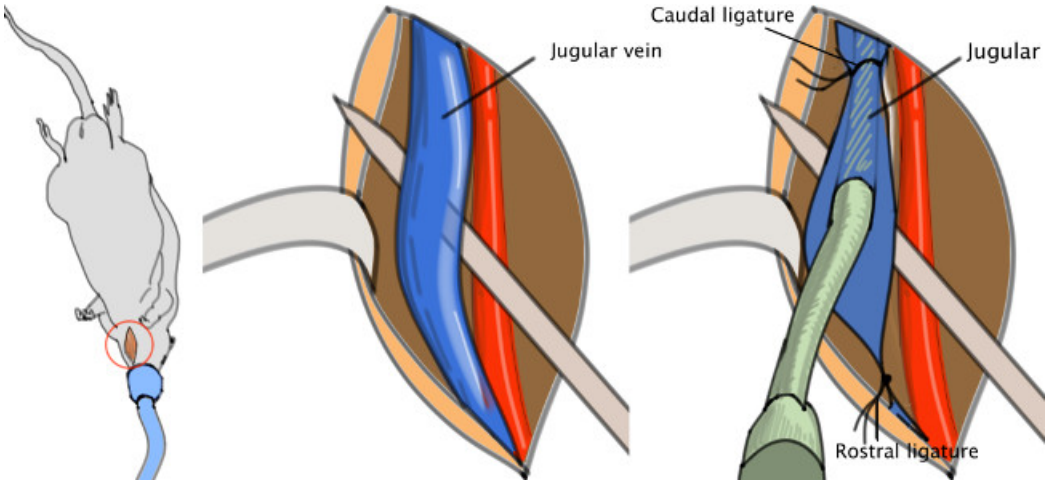

Figure 3. Jugular catheter. The catheter is to be inserted in the jugular vein, then pushed toward the heart and finally fasten with a knot. Please click here to view a larger version of this figure.

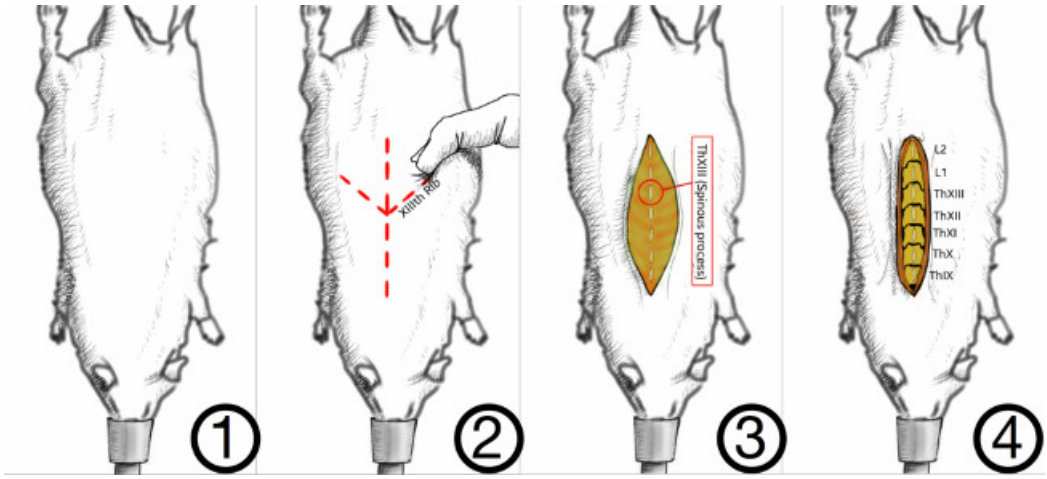

Figure 4. Method for correct identification of the vertebral levels. In the rat, the last rib is attached to the XIIIth vertebra. The latter can be palpated through the skin as a landmark for the last thoracic vertebra, the XIIIth. Muscles are detached on either side of the spinous processes. Please click here to view a larger version of this figure.

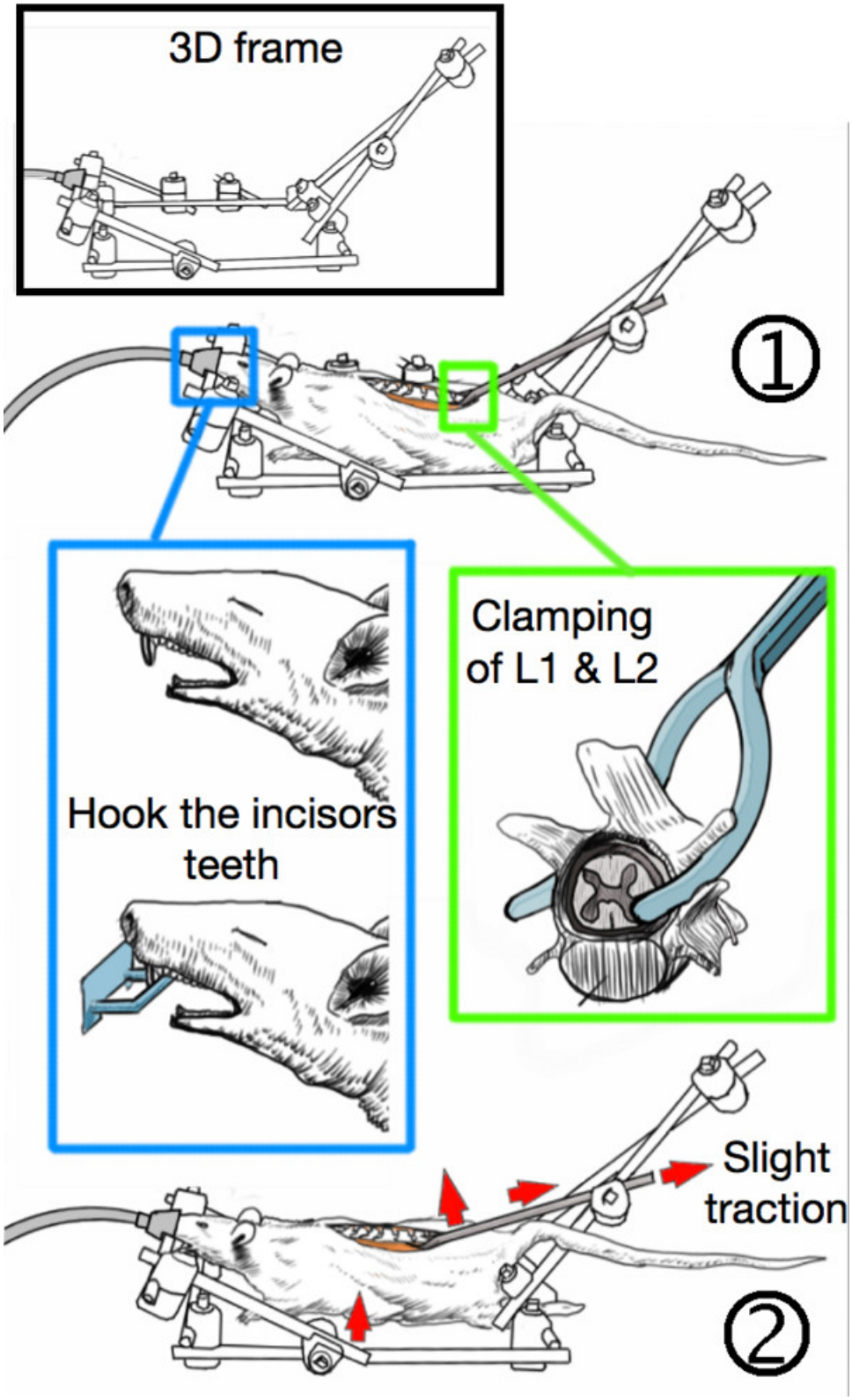

Figure 5. Stabilization of the animal in the 3D-frame. (1) The incisor teeth are hooked on the frame while the first and second lumbar vertebras (L1 & L2) are clamped with custom-made forceps. (2) The lumbar spine is slightly tightened which stabilizes the animal and elevates the thorax from the bench, thereby allowing free respiratory motions without spine movements. Please click here to view a larger version of this figure.

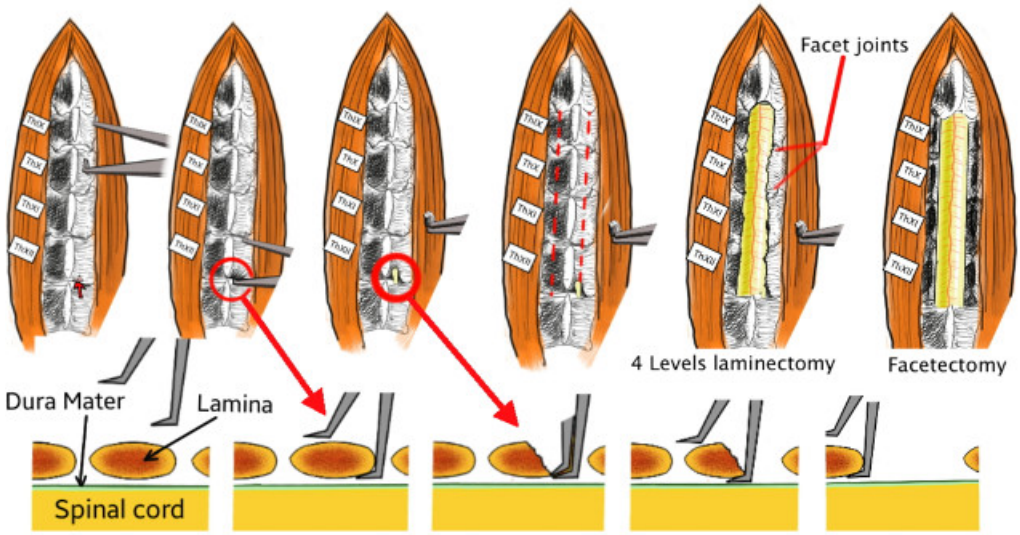

Figure 6. Technical details of the laminectomy. First, the thin blade of the custom-made bone cutter is passed beneath the lamina without damaging the spinal cord. Then the bone cutter is closed, which cuts and removes a part of the lamina. The procedure is repeated on both sides and from ThXII to TxIX in order to achieve a four-level laminectomy. Finally, the facet joints are also removed. Please click here to view a larger version of this figure.

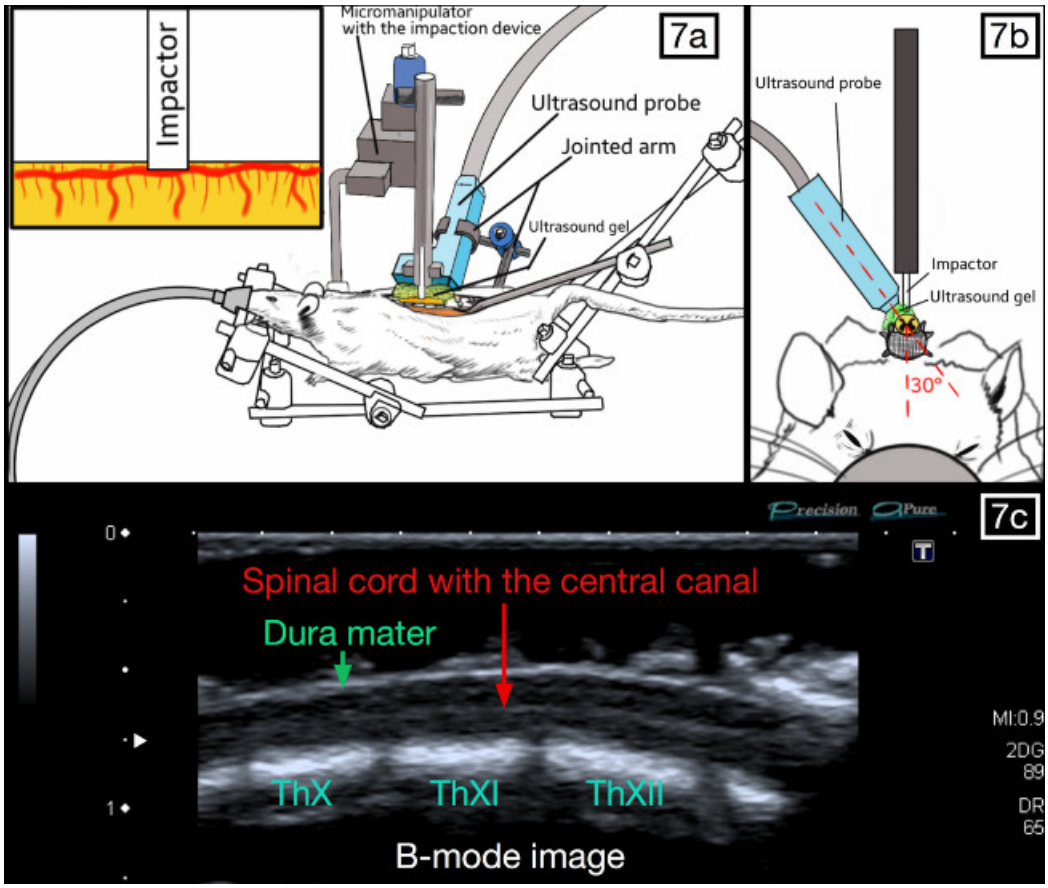

Figure 7. Positioning of the ultrasound probe and the impaction device. The probe is parallel to the spinal cord and slightly oblique (20-30°), so that the weight-drop impactor can be placed against the posterior aspect of the dura. The spinal cord should be visible with the central canal present throughout the middle segment on the ultrasound imaging "B-Mode". Please click here to view a larger version of this figure.

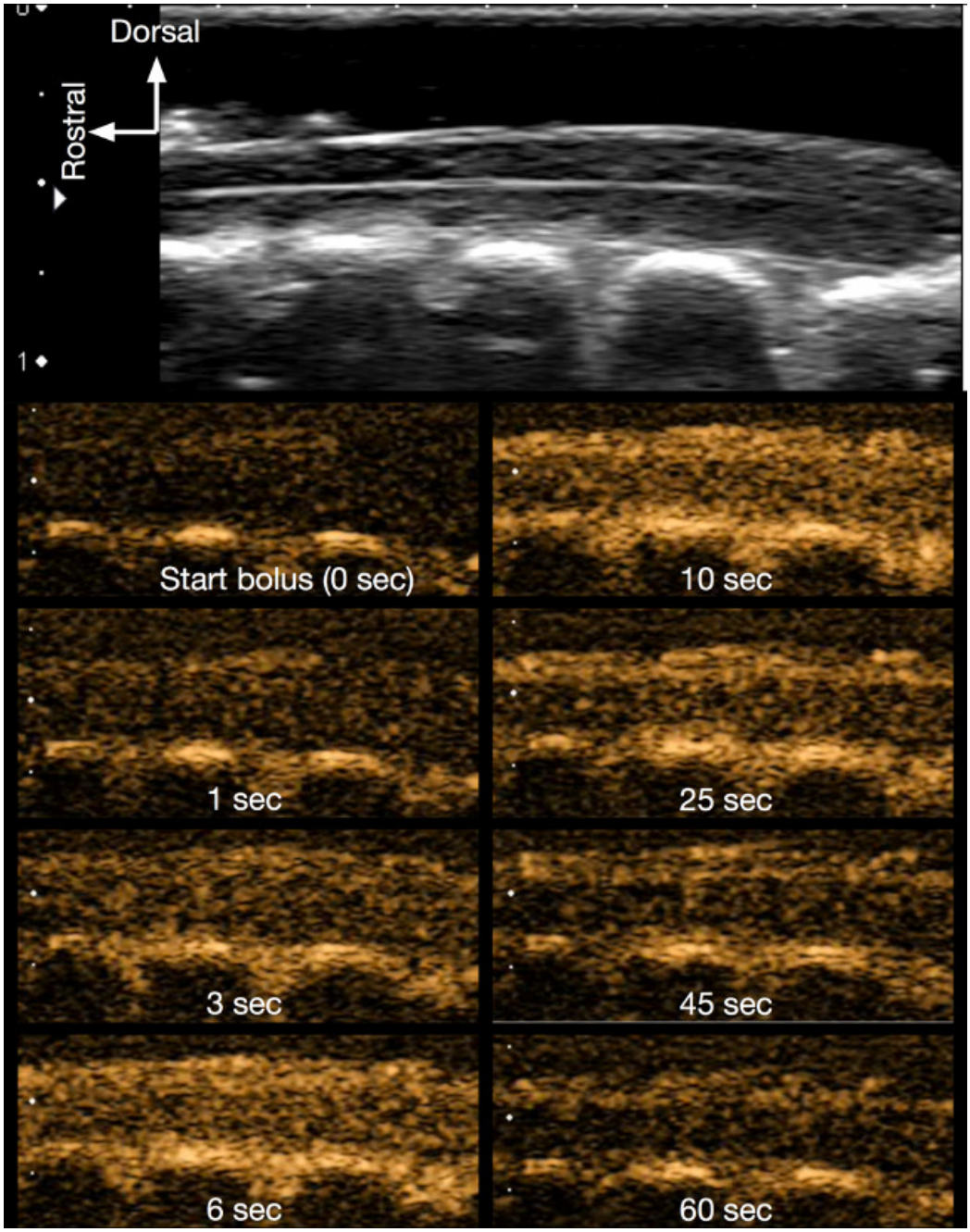

Figure 8. Contrast imaging of the intact spinal cord. The successive figures in contrast mode (orange coloured images) show how the contrast agent (microbubbles) progressively appears following the infusion, thereby enhancing the contrast of the spinal cord. Bolus infusion lasts about 10 sec and the contrast data was recorded for 1 min. Please click here to view a larger version of this figure.

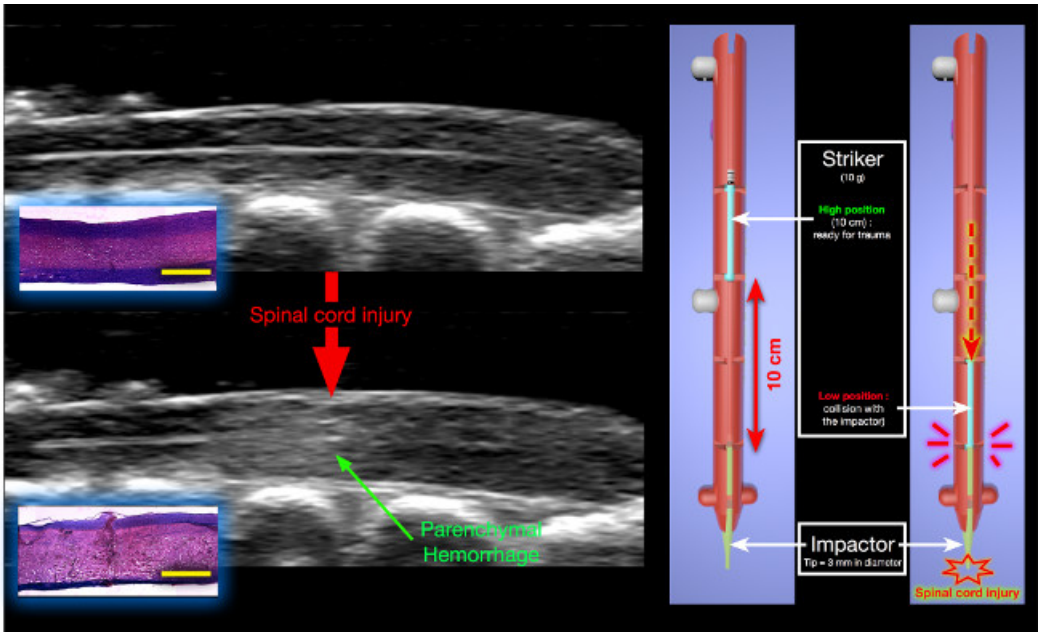

Figure 9. Changes in B-mode following experimental SCI. A hyperechoic lesion appears inside the parenchyma, corresponding to the initial parenchymal hemorrhage post-SCI. Histology (H&E staining) : The hemorrhage results from massive traumatic disruption of small blood vessels leading to blood extravasation in the parenchyma (yellow scale bar = 2,000 µm). The impaction device is shown on the right. The striker is released from a 10 cm height and collides with the impactor that subsequently generates the spinal cord injury. Please click here to view a larger version of this figure.

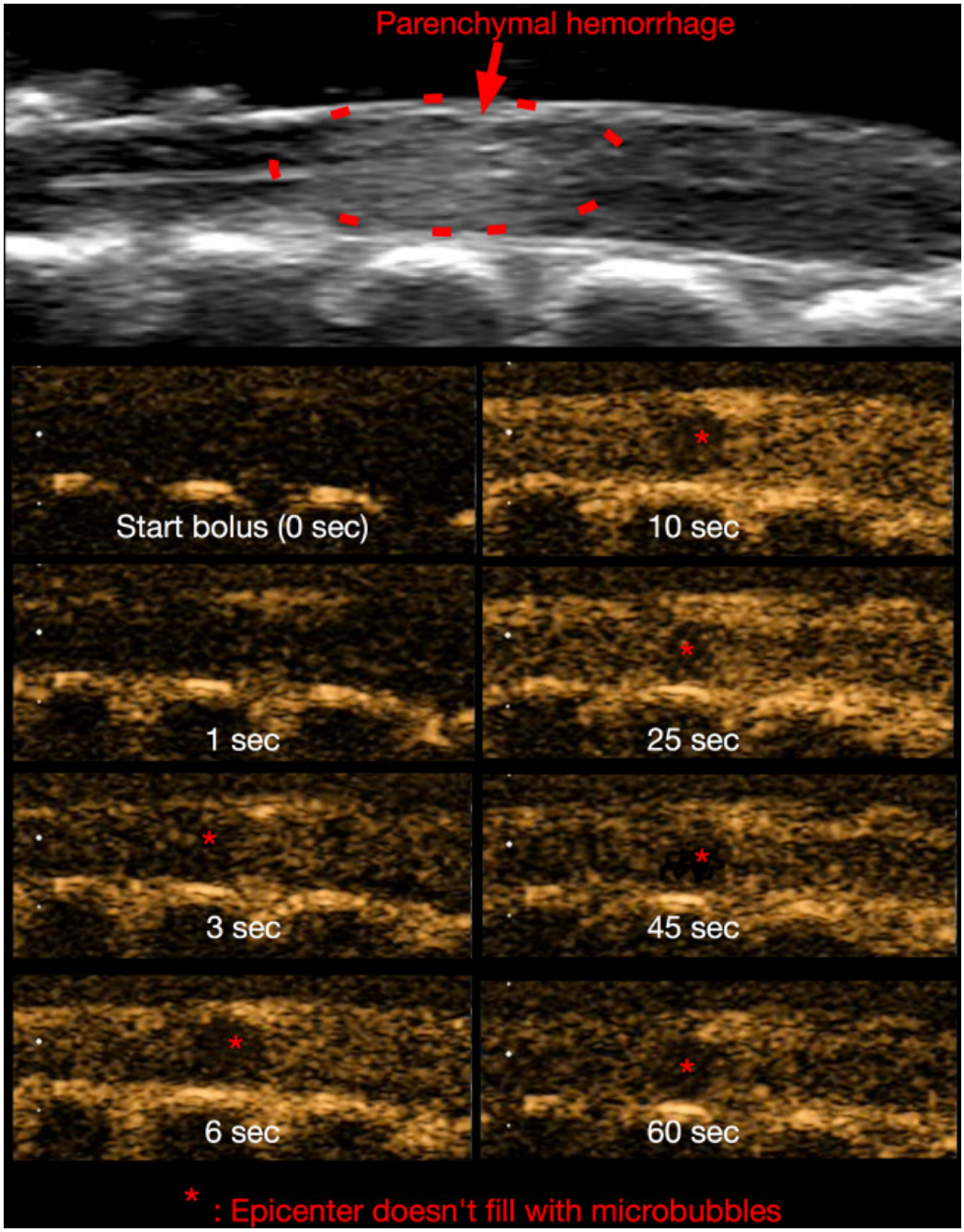

Figure 10. Contrast imaging 15 min post-SCI. Similar to Figure 8, the microbubbles are visible as they pass through the spinal cord microvasculature. At the epicenter (asterisk), the blood flow is obstructed by microvascular disruption. Please click here to view a larger version of this figure.

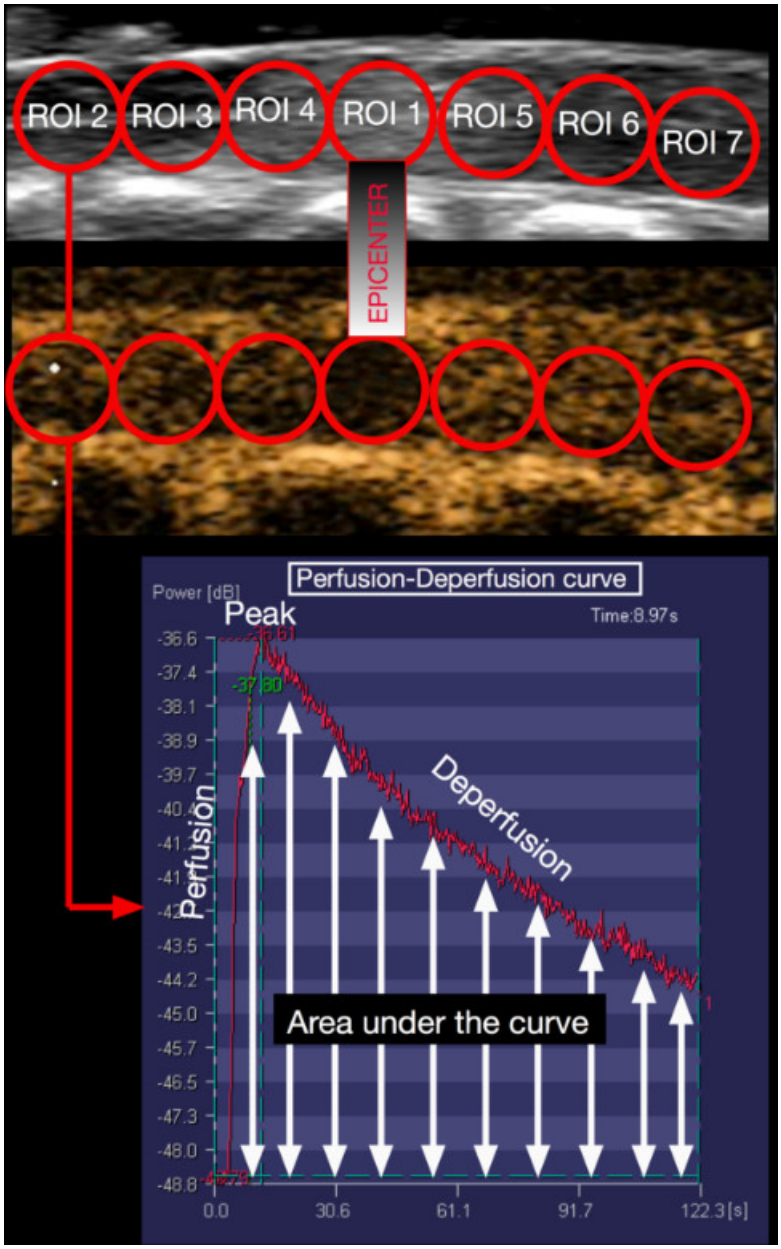

Figure 11. Protocol for SCBF quantification. With Ultra-Extend Software, seven circular and adjacent regions of interest (ROI) are drawn on the longitudinal spinal cord image. The first ROI is placed on the injury epicenter. In each ROI, the software generates a perfusion-deperfusion curve and calculates the area under this curve. This value correlates with the blood flow in this area. Please click here to view a larger version of this figure.

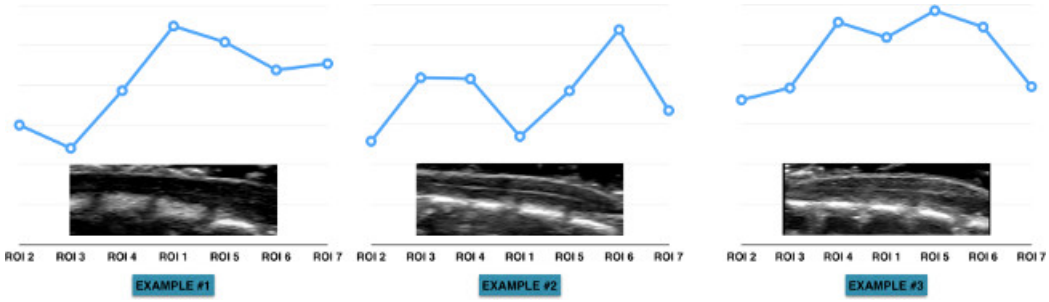

Figure 12. Heterogeneity of the blood flow along the spinal cord. These graphs display the heterogeneity of spinal cord blood flow as well as the variability between animals. This can be largely explained by the vascular anatomy of the spinal cord. However, due to the heterogeneity and variable vascular anatomy, one must use the blood flow measurements (from each ROI) prior to injury as the baseline. The measurements made at the following time-points (post-SCI) are expressed as the percentages change of the baseline. Please click here to view a larger version of this figure.

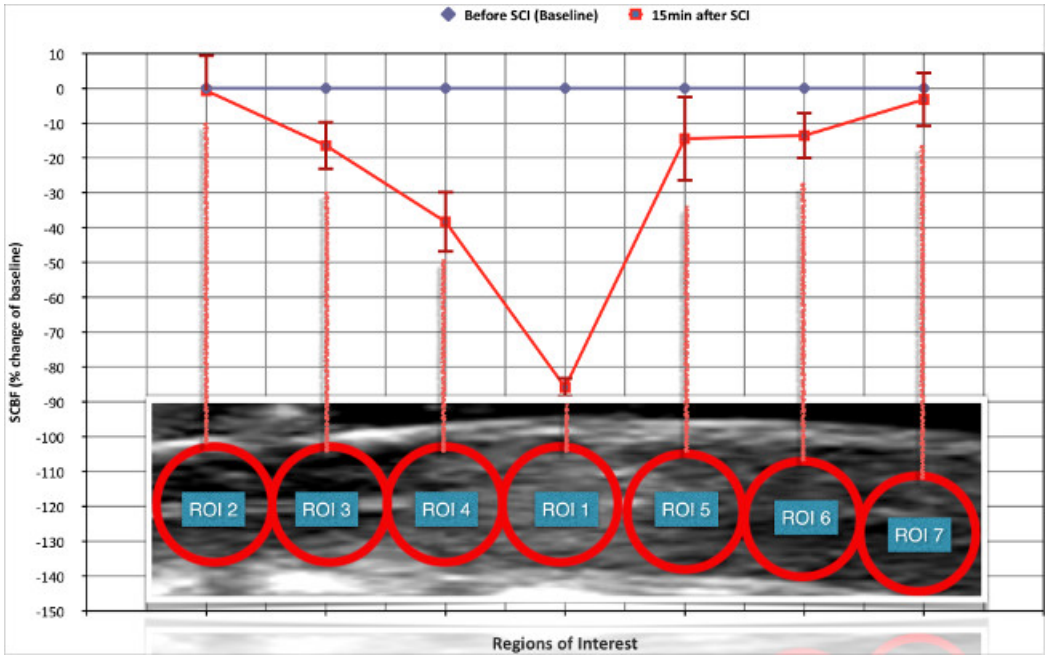

Figure 13. Changes in spinal cord blood flow (SCBF) induced by the experimental spinal cord injury (SCI). 15 min after SCI there is critical ischemia at the level of the epicenter while SCBF remained preserved in the more remote intact areas. In the regions adjacent to the epicenter (both rostral and caudal), SCBF is significantly reduced. This corresponds to the previously described “ischemic penumbra zone”. Please click here to view a larger version of this figure.

Discussion

Although we have described how to use CEU in a rat SCI contusion model, this protocol can be modified to fit other experimental objectives or SCI models. We have chosen to measure SCBF at only two time points (before injury and 15 min post-SCI), however the number of time points and the delay between SCBF measurements can be adapted to fulfill the needs of other studies. For example, in our previous work [17], we have measured SCBF at five successive time points throughout the first hour post-SCI. It is important to note that in the sham group (no SCI), we were surprised to observe a progressive decrease in SCBF. While we initially feared that repeated microbubble infusion might harm the spinal cord vasculature, further experimentation (unpublished data) confirmed that these changes were caused by progressive alterations in local tissue physiological conditions (temperature, hydration) induced by the laminectomy, as well as the prolonged exposition of the dura and surrounding tissue to the ambient air and the ultrasound gel. These problems are common in all experiments dealing with microcirculation, as the circulation is extremely sensitive to many parameters and therefore prone to vascoconstriction or vasodilatation. Therefore, we recommend that the period during which the surgical wound remains open is as short as possible. If multiple SCBF measurements are needed over a prolonged period, it would be preferable to close the animal incision between the acquisitions in order to restore physiological conditions around and inside the spinal cord.

It is also possible to modify the shape, size, location and the number of ROIs for SCBF analysis. One of the major advantages of CEU is that the measurements can be made anytime following experimental completion by processing the recorded data offline. It is also possible to repeat the measurements or to modify the measurement settings/standards if necessary.

In the protocol described here, we applied a contusion model of SCI. However, there are other models, including clip compression or cord transection [21] that can be easily adapted to measure SCBF with this protocol. Once the spinal cord is injured, one simply needs to place the

ultrasound gel on the dura mater and position the ultrasound probe. We also choose to measure SCBF at the lower thoracic level because it corresponds to the model that we currently use in our lab. However, the same technique can be used at other levels of the spinal cord. Since the whole spine is stabilized between the lumbar spine (clamping at L2) and the incisors teeth, one simply needs to make a laminectomy at the desired level and position the probe accordingly.

Spatial resolution of ultrasound imaging is proportional to the frequency of the ultrasound waves. The higher the ultrasound frequency, the better the spatial resolution. We have used a high-frequency (12-14 MHz) probe, which provides an image with a pixel resolution of about 100 µm. With very-high-resolution systems, the frequency increases up to 55 MHz and each pixel is about 20 µm [20]. Such devices can also be used for CEU, which depict much more precisely the distribution of SCBF in the parenchyma. However, the very-high-resolution systems are much more expensive.

Several other techniques have been proposed to measure SCBF in SCI, but they all have unique limitations. Some, such as radioactive microspheres[7,8] or the C14-iodo-antipyrine autoradiography[9], require animal sacrifice. In these cases, the spinal cord must be harvested for analysis. On the other hand, the hydrogen clearance technique[10], requires intraspinal electrode insertion which may actually modify the SCBF. Moreover, the measurement can only be made in a very restricted region of the spinal cord parenchyma. Light microscopy through a spinal window also provides a way to assess microcirculation, but this approach has a very restricted depth of observation. It only allows to observe the circulation in the superficial pia matter and not within the parenchyma [16].

In literature, real time *in-vivo* assessments of SCBF are usually performed by laser Doppler imaging [11-13]. However, even this technique has several limitations. Firstly, since the laser is less than 1 mm in diameter, SCBF can only be assessed in a very restricted area corresponding to a semi-sphere of about 1 mm in diameter. Since the rat's spinal cord is about 3 mm in diameter, the limited area of analysis is a major constraint. Moreover, as we have shown that SCBF in the intact spinal cord is not homogeneous, it is important to measure SCBF in a larger area for a proper representation of tissue microcirculation. Secondly, the laser has a limited depth of penetration and therefore detects superficial SCBF. As a result, it not only measures parenchymal SCBF but also that of the pia mater (that surrounds the parenchyma). Since the pia mater has a unique vascular system and is not subjected to the same auto-regulatory mechanisms as parenchymal vessels, this information may be misleading. Lastly, the laser-Doppler doesn't provide any morphological information. CEU overcomes such limitations by displaying morphological images of the cord (B-mode), while uniquely presenting the contrast agent that can be clearly identified within the parenchyma.

Despite its many advantages to other approaches, CEU also has some distinct limitations. Since measurements are made on a bi-dimensional sagittal slice (usually parallel to the central canal), SCBF from other regions of the parenchyma are inaccessible. Further, the information generated by a single bi-dimensional sagittal spinal cord segment may not be representative of the entire cord. Nevertheless, this can be controlled by several precautions. First, by repeating measurements at the same location, the first measurement made (intact spinal cord) can be used as a baseline value. Second, by injuring at the spinal cord midline (bilateral injury), the SCBF changes should be symmetrical between left and right (unpublished data). These precautions help ensure that analysis of single sagittal slice is enough to reflect the global longitudinal distribution of SCBF.

The high cost of ultrasound machines is another limitation. However, several solutions exist to target this problem. First, some labs can negotiate a temporary loan by the manufacturer for their experiments. As ultrasound machines are transportable, temporary loans are possible. This has been the approach used by our lab. Alternatively, a group of labs can pool resources to buy the machine and split the costs. Otherwise, many university institutions have imaging facilities and ultrasound machines can be recommended as essential tools. Thus, animals can be transported the imaging facility for CEU assessment and then brought back for other experiments.

To assess vascular changes, contrast agent (microbubbles) must be injected intravenously. Although catheterization of the jugular or femoral vein is invasive and risky, the veins are easily accessible and clearly identifiable. In contrast, tail vein injection is much less invasive, but the vessel is poorly distinguished/visible for proper catheterization. Therefore, there is a risk that the needle tip will not be properly placed inside the vein or that it may move during injection, compromising the entire experiment. For such reason, we prefer to use the jugular vein and introduce a catheter for consistent microbubble infusion.

Vertebra bones surround the spinal cord. As ultrasound waves are reflected by bone and cannot pass through the spinal cord laminas, imaging requires bone removal (laminectomy) to open an acoustic window. The easiest way to open the vertebral canal is to remove the posterior arch of the vertebra through a laminectomy. In this protocol, we require a four-level laminectomy to visualize a long segment of spinal cord, including the epicenter, the penumbra zone and remote areas of intact spinal cord. Although a majority of experimental SCI models require a laminectomy (for clip application or impactor contusion), these usually consist of removing 1-2 lamina. The extensive 4-level laminectomy is another limitation of our study. However, if one only needs to study the epicenter and penumbra zone, a less extensive laminectomy can be made and is recommended.

In conclusion, despite the several limits described above, CEU is a useful tool for assessing SCBF changes and the effect of various therapies (research purposes). This reliable, real-time, *in-vivo* approach is ideal for looking at treatments to reduce ischemia and subsequent tissue necrosis post-SCI.

Disclosures

The authors declare that they have no competing financial conflict of interest. The ultrasound machine was graciously lent by the Toshiba France company. The Vueject pump was graciously lent by the Bracco France company.

Acknowledgements

We acknowledge Stephanie Gorgeard, Thierry Scheerlink (Toshiba France), and Christophe Lazare (Bracco France).

References

1. Cadotte, D. W., Fehlings, M. G. Spinal cord injury: a systematic review of current treatment options. *Clin Orthop Relat Res.* **469**, (3), 732-741 (2011).
2. Beattie, M. S., Farooqui, A. A., Bresnahan, J. C. Review of current evidence for apoptosis after spinal cord injury. *J Neurotrauma.* **17**, (10), 915-925 (2000).
3. MacDonald, J. W., Sadowsky, C. Spinal-cord injury. *Lancet.* **359**, (9304), 417-425 (2002).
4. Mautes, A. E., Weinzierl, M. R., Donovan, F., Noble, L. J. Vascular events after spinal cord injury: contribution to secondary pathogenesis. *Phys Ther.* **80**, (7), 673-687 (2000).
5. Martirosyan, N. L., *et al.* Blood supply and vascular reactivity of the spinal cord under normal and pathological conditions. *J Neurosurg Spine.* **15**, (3), 238-251 (2011).
6. Blight, A. R. Cellular morphology of chronic spinal cord injury in the cat: analysis of myelinated axons by line-sampling. *Neuroscience.* **10**, (2), 521-543 (1983).
7. Bassingthwaighte, J. B., *et al.* Validity of microsphere depositions for regional myocardial flows. *Am J Physiol.* **253**, (1 Pt 2), H184-H193 (1987).
8. Drescher, W. R., Weigert, K. P., Bunger, M. H., Hansen, E. S., Bunger, C. E. Spinal blood flow in 24-hour megadose glucocorticoid treatment in awake pigs. *J Neurosurg.* **99**, (3 Suppl), 286-290 (2003).
9. Golanov, E. V., Reis, D. J. Contribution of oxygen-sensitive neurons of the rostral ventrolateral medulla to hypoxic cerebral vasodilatation in the rat. *J Physiol.* **495**, (Pt 1), 201-216 (1996).
10. Ueda, Y., *et al.* Influence on spinal cord blood flow and function by interruption of bilateral segmental arteries at up to three levels: experimental study in dogs). *Spine (Phila Pa 1976).* **30**, (20), 2239-2243 (2005).
11. Carlson, G. D., *et al.* Sustained spinal cord compression: part II: effect of methylprednisolone on regional blood flow and recovery of somatosensory evoked potentials). *J Bone Joint Surg Am.* **85-A**, (1), 95-101 (2003).
12. Hamamoto, Y., Ogata, T., Morino, T., Hino, M., Yamamoto, H. Real-time direct measurement of spinal cord blood flow at the site of compression: relationship between blood flow recovery and motor deficiency in spinal cord injury. *Spine (Phila Pa 1976).* **32**, (18), 1955-1962 (2007).
13. Horn, E. M., *et al.* The effects of intrathecal hypotension on tissue perfusion and pathophysiological outcome after acute spinal cord injury). *Neurosurg Focus.* **25**, (5), E12 (2008).
14. Phillips, J. P., George, K. J., Kyriacou, P. A., Langford, R. M. Investigation of photoplethysmographic changes using a static compression model of spinal cord injury. *Conf Proc IEEE Eng Med Biol Soc.* **2009**, 1493-1496 (2009).
15. Phillips, J. P., George, K. J., Kyriacou, P. A., Langford, R. M. Investigation of photoplethysmographic changes using a static compression model of spinal cord injury. *Conf Proc IEEE Eng Med Biol Soc.* **2009**, 1493-1496 (2009).
16. Ishikawa, M., *et al.* Platelet adhesion and arteriolar dilation in the photothrombosis: observation with the rat closed cranial and spinal windows. *J Neurol Sci.* **194**, (1), 59-69 (2002).
17. Soubeyrand, M., *et al.* Real-time and spatial quantification using contrast-enhanced ultrasonography of spinal cord perfusion during experimental spinal cord injury. *Spine (Phila Pa 1976).* **37**, (22), E1376-E1382 (1976).
18. Huang, L., *et al.* Quantitative assessment of spinal cord perfusion by using contrast-enhanced ultrasound in a porcine model with acute spinal cord contusion). *Spinal Cord.* **51**, (3), 196-201 (2012).
19. Postema, M., Gilja, O. H. Contrast-enhanced and targeted ultrasound. *World J Gastroenterol.* **17**, (1), 28-41 (2011).
20. Soubeyrand, M., Badner, A., Vawda, R., Chung, Y. S., Fehlings, M. Very High Resolution Ultrasound Imaging for Real-Time Quantitative Visualisation of Vascular Disruption After Spinal Cord Injury. *J Neurotrauma.* (2014).
21. Akhtar, A. Z., Pippin, J. J., Sandusky, C. B. Animal models in spinal cord injury: a review. *Rev Neurosci.* **19**, (1), 47-60 (2008).